Supporting Information

Ligand-Asymmetric *Janus* Quantum Dots for Efficient Blue-Quantum Dot Light-Emitting Diodes

Ikjun Cho,[†] Heeyoung Jung,[‡] Byeong Guk Jeong,[⊥] Donghyo Hahm,[#] Jun Hyuk Chang,[#] Taesoo Lee,[‡] Kookheon Char,[#] Doh C. Lee,[⊥] Jaehoon Lim,[§] Changhee Lee,[‡] Jinhan Cho[*,†] and Wan Ki Bae*[*,¶]

†Department of Chemical and Biological Engineering, Korea University, Seoul 02841, Republic of Korea

‡School of Electrical and Computer Engineering, Inter-University Semiconductor Research Center, Seoul National University, Seoul 08826, Republic of Korea

⊥Department of Chemical and Biomolecular Engineering, Korea Advanced Institute of Science and Technology (KAIST), Daejeon 34141, Republic of Korea

School of Chemical and Biological Engineering, The National Creative Research Initiative Center for Intelligent Hybrids, Seoul National University, Seoul 08826, Republic of Korea

§Department of Chemical Engineering, Ajou University, Seongnam-si, Geyong gi-do 13559, Republic of Korea

¶ SKKU Advanced Institute of Nano Technology (SAINT), Sungkyunkwan University, Seobu-ro, Jangan-gu, Suwon-si, Gyeong gi-do 16419, Republic of Korea

Corresponding Author

***E-mail: chlee7@snu.ac.kr, jinhan71@korea.ac.kr, and wkbae@skku.edu**

1. Experimental methods

Chemicals: Zinc acetate ($Zn(acet)_2$, 99.99%, metals basis), 1-octadecene (ODE, 90%) and tri-n-octylphosphine (TOP, ≥ 99%) were purchased from UniAm (Korea). Cadmium oxide (CdO, 99.95%, metals basis), S (99.998%, powder), oleic acid (OA, 90%), 1-dodecanethiol (DDT, ≥98%), and myristic acid (MA, ≥ 99%) were obtained from Alfa Aesar. Poly(amidoamine) dendrimer generation 0 (PAD), and dodecylamine (DA, 99.9%) were acquired from Sigma-Aldrich. All organic solvents were used as received from Daejung (Korea) without purification.

Preparation of Precursors: Preparation of Cationic precursors (0.5 M cadmium oleate [$Cd(OA)_2$] and 0.5 M zinc oleate [$Zn(OA)_2$)] was conducted with a typical Schlenk line technique under Ar condition. For $Cd(OA)_2$ [or $Zn(OA)_2$], 100 mmol of CdO [or $Zn(acet)_2$], 100 mL of OA and 100 mL of ODE were loaded in 250 mL three-neck flask. The reaction flask was degassed at 110 ºC for 3 hr, followed by back-filling with Ar. Then, the flask was heated up to 250 ºC for 1 hr, and back-filled with Ar. Anionic precursors [0.5 M sulfur dissolved in octadecene (S-ODE)] were prepared under inert atmosphere. 40 mmol of sulfur power and 80 mL of ODE were mixed in 100 mL of three-neck flask. The flask was heated up 100 ºC for 1 hr under Ar atmosphere.

Synthesis of Blue QDs: CdZnS(r = 2 nm)/ZnS(h = 2.3 nm) blue QD were synthesized by modified synthetic methods.[S1] 1 mmol of CdO, 10 mmol of $Zn(acet)_2$ and 7 mL of OA were degassed in the three-neck flask at 140 ºC for 1 hr. After back-filling of Ar, 15 mL of ODE was added and degassed at 110 ºC for 1 hr. Then, the reaction flask was heated to 310 ºC to form a clear mixture solution of $Cd(OA)_2$ and $Zn(OA)_2$ under Ar atmosphere. 3 mL of S-ODE solution was injected swiftly in the reaction flask. After 10 min of reaction, 16 mL of S-

ODE solution was injected dropwise at the rate of 2 mL/min for the ZnS shelling. The reaction temperature was maintained at 310 ºC for 1 hr. The resultant QDs were purified three times *via* the precipitation/redispersion method and redispersed in toluene for further uses.

Synthesis of ZnO nanoparticles: ZnO nanoparticles (NPs) were synthesized *via* a modification of previously reported methods.[S2] 1.23 g of $Zn(acet)_2 \cdot 2H_2O$ was dissolved in 55 mL of methanol at room temperature. Then, 25 mL of a methanol solution containing 0.48 g of KOH was added dropwise at 60 ºC with magnetic stirring. The reaction mixture was kept at 60 ºC for 2 hr under N_2 atmosphere. The product appeared as white precipitate. After collecting by centrifugation, this white precipitate was washed with methanol. Finally, 0.1 mL of butylamine was added for stabilization and the precipitate was redispersed in butanol (20 mg/mL).

Device fabrication*:* Prepared ZnO NPs solution was spun-cast on patterned ITO substrates with a spin rate of 2000 rpm for 40 s to form ZnO films. PAD ligand layers were formed on the ZnO film as the bottom ligands (BL) by spin-casting PAD ligand solutions diluted in methanol (2 mg/mL) with a spin-rate of 4000 rpm for 30 s. The weakly bound PAD ligands were washed by spin-casting PAD//ZnO substrates with pure methanol under the same spin condition. QD dispersions (20 mg/mL in toluene) were then deposited on PAD//ZnO substrates at 4000 rpm for 30 s, followed by a washing step (spin-casting with pure toluene). Then dodecylamine (DA) ligand solution was spun coated exchanging top ligand to control the surface energy of QD emissive layer ((OA/QD/PAD)//ZnO). mCP or CBP, MoO_x, and Al electrode layers were thermally evaporated under a vapor pressure of 1×10^{-6} torr onto

(DA/QD/PAD)//ZnO//ITO substrates at deposition rates of 1 Å/s, 0.2 Å/s, and 4–5 Å/s, respectively.

Optical Characterization: UV-vis absorption and photoluminescence spectra were obtained with a Lambda 35 spectrometer (PerkinElmer) and Fluoromax-4 spectrometer (Horiba Science), respectively. The measurements for characterizing the PL decay dynamics were done with a time-correlated single-photon counting (TCSPC) system from Horiba-Jovin Yvon, which has resolution of about 100 ps. The samples were measured with excitation at 3.1 eV and a repetition rate of 200 kHz.

Film Characterization: The adsorption of PAD, (OA/QD/OA), QDs onto PAD-coated substrates (OA/QD/PAD), and the dodecylamine ligand (DA) onto modified QD layers (DA/QD/PAD) were qualitatively investigated using fourier transform infrared spectroscopy (FT-IR) in attenuated total reflection (ATR) mode (Agilent Technologies Cary 600 Series). The surface morphologies of the films (*i.e.*, CBP//(OA/QD/PAD)//ZnO, mCP//(OA/QD/OA)//ZnO and mCP//(DA/QD/PAD)//ZnO) were investigated with non-contact mode of atomic force microscopy (AFM) (XE-100, Park System). Ultraviolet photoelectron spectroscopy (UPS) measurements were conducted with an AXIS-NOVA and Ultra DLD using a He I (21.2 eV for UPS) discharge lamp. The contact angles of QDs onto ZnO substrates were measured by the sessile drop method using a contact angle measurement system (Pheonix-300, SEO Corporation) equipped with a video capture apparatus. The surface energy were calculated by the Owen-Wendt method using Young's equation (1), Owne-Wendt equation (2) and equation (3).[S3,S4]

$\gamma_{SG} = \gamma_{SL} + \gamma_{LG}\cos\theta$ (1) (Young's equation)

$\gamma_{SL} = \gamma_{SG} + \gamma_{LG} - 2\left(\gamma_{SG}^{d} \cdot \gamma_{LG}^{d}\right)^{\frac{1}{2}} - 2(\gamma_{SG}^{p} \cdot \gamma_{LG}^{p})^{1/2}$ (2) (Owen-Wendt equation)

$\gamma_{SG} = \gamma_{SG}^{d} + \gamma_{SG}^{p}$ (3)

Where γ_{LG} is the surface energy of liquid and gas, γ_{SG} is the surface energy between solid materials and gas, γ_{SG}^{d} is the dispersion component of surface energy and γ_{SG}^{p} is the polar component of surface energy. To determine the surface energy, two measure liquids, for example deionized water (DI) and ethylene glycol (EG), whose surface energy and polar and dispersion components of surface energy are known are used. The polar component of DI is 51 mJ/m^2 with total surface energy 72.8 mJ/m^2 and the polar component of EG is 19 mJ/m^2 with total surface energy 48 mJ/m^2. In order to calculate the surface energy of the analyzed materials (CBP, mCP, and QD films with ligands), the contact angles (θ) with the DI and EG were measured. Then, we obtained γ_{SG} from solving the equation (1), (2), and (3).

Device Characterization of QLEDs: The current–voltage–luminance (I–V–L) characteristics of the devices were measured with a Keithley-236 source-measure unit, a Keithley-2000 multimeter unit coupled with a calibrated Si photodiode (Hamamatsu S5227-1010BQ) and a photomultiplier tube detector. The luminance and efficiencies of QLEDs were calculated from the photocurrent measurement data obtained with the Si photodiode. The electroluminescence spectra were obtained using a spectroradiometer (CS-2000).

Device Simulation of QLEDs: The device simulator SimOLED (v4.2.1) models the electrical behavior of QLED devices by assuming electrical properties of quantum dot as organic materials.[S5] The draft-diffusion equation is solved based on the 1-D finite element method (FEM) for holes and electrons and the involved excitons.[S6,S7] Followed Poisson equation, continuity equations are numerically solved using FEM.

$\frac{\partial F}{\partial x} = \frac{q}{\varepsilon\varepsilon_0}(p(x,t) + n(x,t))$ (4)

$$\frac{\partial n_f(x,t)}{\partial t} = \frac{1}{q}\frac{\partial J_{nf}(x,t)}{\partial x} - R - T \quad (5)$$

$$\frac{\partial s(x,t)}{\partial t} = \mathrm{c} \cdot \mathrm{R} + D_s\frac{\partial s(x,t)}{\partial x} - \frac{s(x,t)}{\tau_s} - Q \quad (6)$$

Poisson equation is expressed as equation (4), while F is the electric field inside the QLEDs, q is the elementary charge, ε is the dielectric permittivity of the organic materials, ε_0 is the dielectric constant, p and n are the charge carrier concentrations for holes and electrons (includes free and trapped charges), respectively. Continuity equation for electron is stated as equation (5), whereas n_f is the charge carrier concentration of free electrons, J_{nf} is the electron current density, R is the recombination rate (between free and between free and trapped carriers), T is the trapping rate for free carriers. Therefore, exciton density s is formulated in equation (6) whilst c is a factor due to spin statistics (1/4 for singlet, 3/4 for triplet), D_s is the diffusion constant for excitons, τ_s is the exciton lifetime, and Q is includes quenching terms for excitons (*i.e.* quenching at contacts, free carriers or excitons).

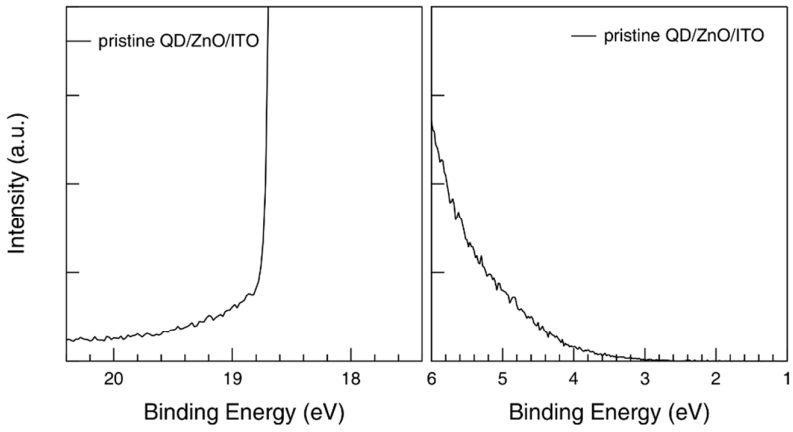

Figure S1. UPS spectra at the high binding energy regime (left) and at the low binding energy regime (right) of the pristine QD (*i.e.*, (OA/QD/OA)//ZnO//ITO) films. The valance band edge (VBE) and conduction band edge (CBE) energy levels of pristine CdZnS(r = 2 nm)/ZnS(h = 2.3 nm) QD layers are 6.95 eV and 4.19 eV, respectively.

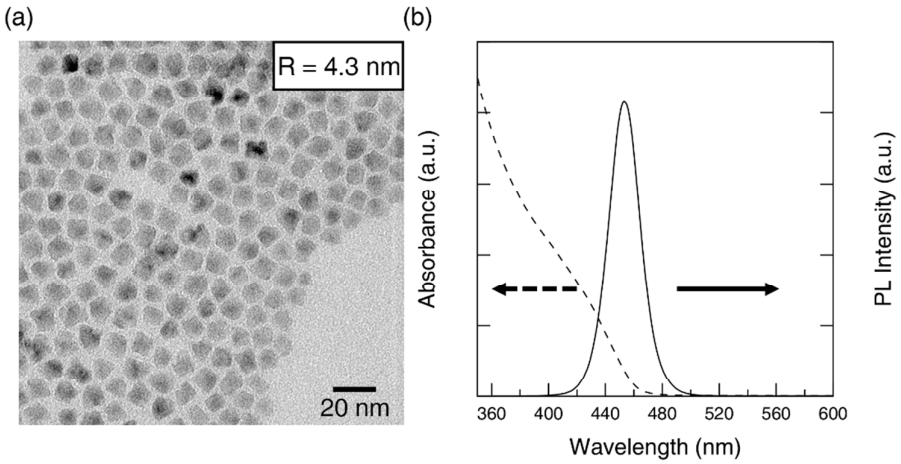

Figure S2. Characteristics of blue CdZnS(r = 2 nm)/ZnS(h = 2.3 nm) QDs. (a) High-resolution TEM image, and (b) UV absorbance and PL spectra of of CdZnS(r = 2 nm)/ZnS(h = 2.3 nm) blue QDs.

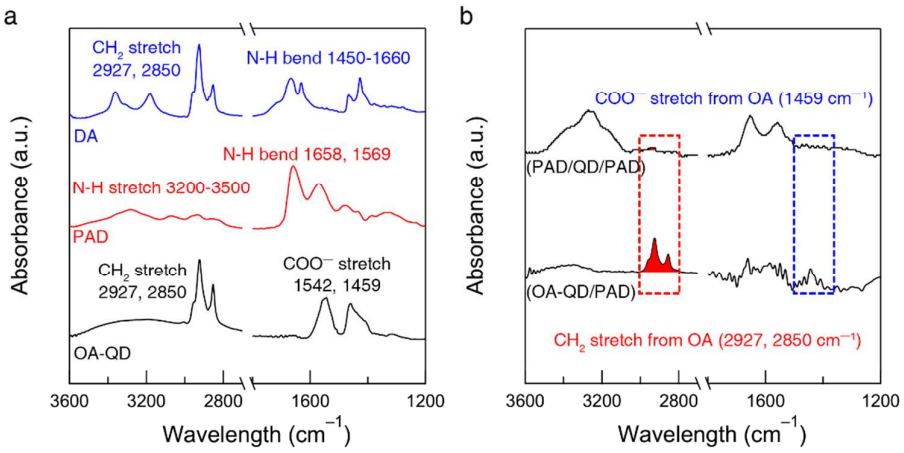

Figure S3. (a) FT-IR spectra of oleic acid capped QD (OA-QD), poly(amidoamine) dendrimers (PAD), and dodecyl amine (DA). The COO^- symmetric stretching peak (at 1459 and 1542 cm^{-1}) and CH_2 stretching peak (at 2850 and 2927 cm^{-1}) by OA stabilizers, the N–H bending peak (at 1569 and 1658 cm^{-1}) by PAD BL, and the N–H bending vibrations (at 1450 ~ 1660 cm^{-1}) by DA TL are assigned in these spectra.[S8,S9] (b) FT-IR spectra of (OA-QD/PAD) and (PAD/QD/PAD) films. The two noticeable peaks (*i.e.*, COO^- stretching peak at 1459 cm^{-1} and CH_2 stretching peak at 2850 and 2927 cm^{-1}) originating from native OA ligands almost disappeared after deposition of PAD onto (OA-QD/PAD) film. These results evidently indicate the ligand exchange between OA and PAD during PAD deposition step. Additionally, when the integrated area of CH_2-stretching peak (by OA) was calculated before and after PAD deposition, a degree of ligand exchange from OA to PAD was measured to be approximately 93 %.

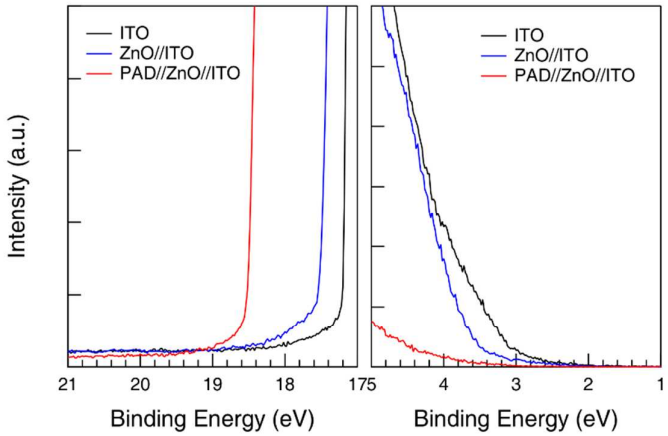

Figure S4. UPS spectra at the high binding energy regime (left) and at the low binding energy regime (right) of (a) the bare ITO films, ZnO//ITO films, and PAD//ZnO//ITO films. The electronic energy level shifts of ZnO layer by amine-functionalized ligands were previously reported.[S9]

Table S1. The electronic energy levels of the surface of ZnO//ITO, PAD//ZnO//ITO, (OA/QD/PAD)//ZnO//ITO, and (DA/QD/PAD)//ZnO//ITO films.

Films	VBE [eV]	CBE [eV]
ZnO//ITO	7.27	4.03
PAD//ZnO//ITO	6.79	3.55
(OA/QD/PAD)//ZnO//ITO	6.93	4.17
(DA/QD/PAD)//ZnO//ITO	6.91	4.15

Abbreviations: valance band edge (VBE) and conduction band edge (CBE).

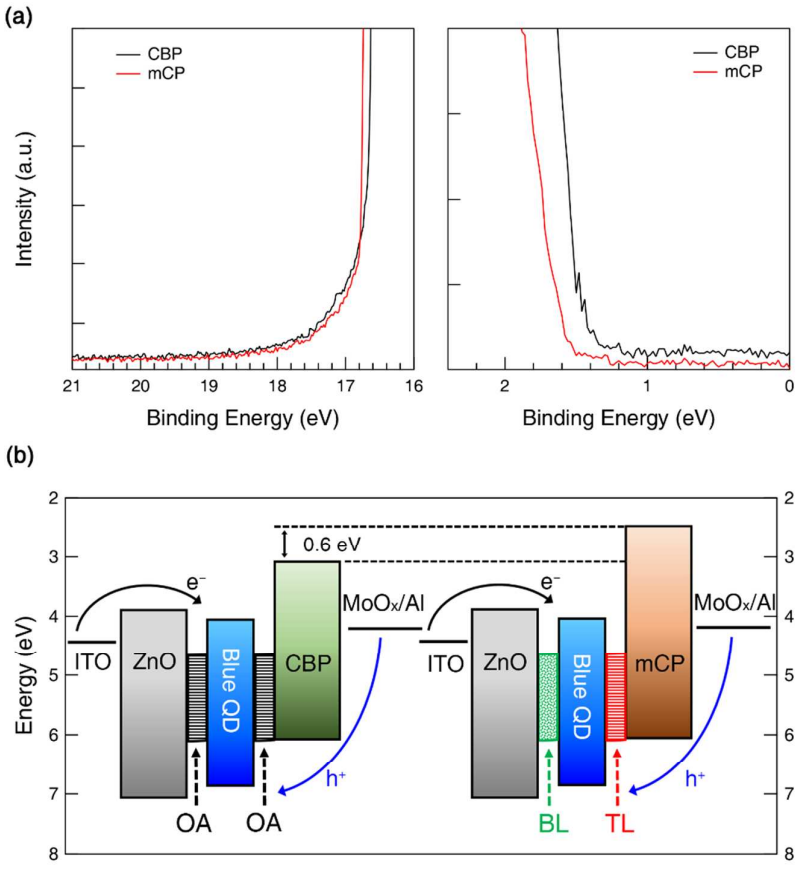

Figure S5. (a) UPS spectra at the high binding energy regime (left) and at the low binding energy regime (right) of the 1,3-bis(N-carbazolyl)benzene (mCP) and 4,4'-bis(N-carbazolyl)-1,1'-biphenyl (CBP). The highest occupied molecular orbital (HOMO) energy level and lowest unoccupied molecular orbital (LUMO) energy level of mCP are 5.99 eV and 2.39 eV, respectively. The HOMO and LUMO energy level of CBP are 6.01 eV and 3.01 eV, respectively. (b) Energy band diagrams of blue QLED employing CBP on QDs with native ligands (*i.e.*, (OA/QD/OA)) *versus* (e) mCP on ligand asymmetric QDs (*i.e.*, (TL/QD/BL)).

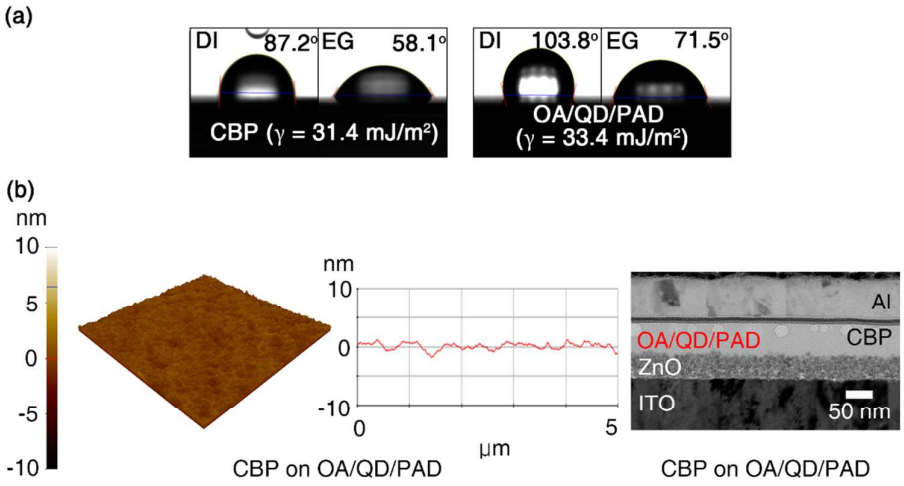

Figure S6. (a) Contact angle images with DI water (DI, left) and ethyleneglycol (EG, right) and the calculated surface energy (γ) of CBP film. (b) Atomic force microscopy images (left) and their height profiles (middle, scan range: 5 μm x 5 μm) of CBP evaporated on QDs with OA and PAD ligands (CBP on (OA/QD/PAD)). Cross-sectional TEM images (right) of QLEDs incorporating CBP on QDs with native ligands and PAD ligands (CBP on (OA/QD/PAD)).

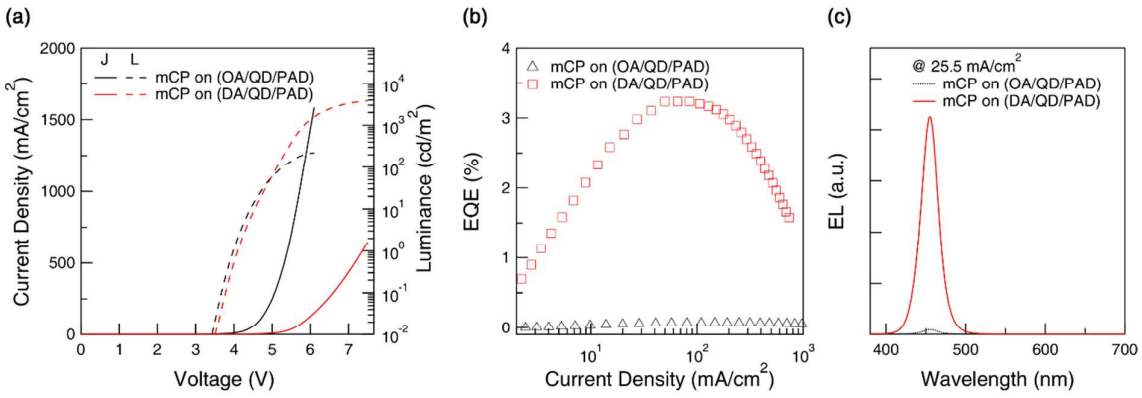

Figure S7. (a) Current density−voltage−luminance characteristics, (b) external quantum efficiency (EQE) *versus* current density and (c) electroluminescence spectra (at a current density of 25.5 mA/cm^2) of QLEDs employing mCP layers deposited on CdZnS(r = 2 nm)/ZnS(h = 2.3 nm) blue QDs passivated with native top ligands (mCP on (OA/QD/PAD), black) *versus* exchanged top ligands (mCP on (DA/QD/PAD), red).

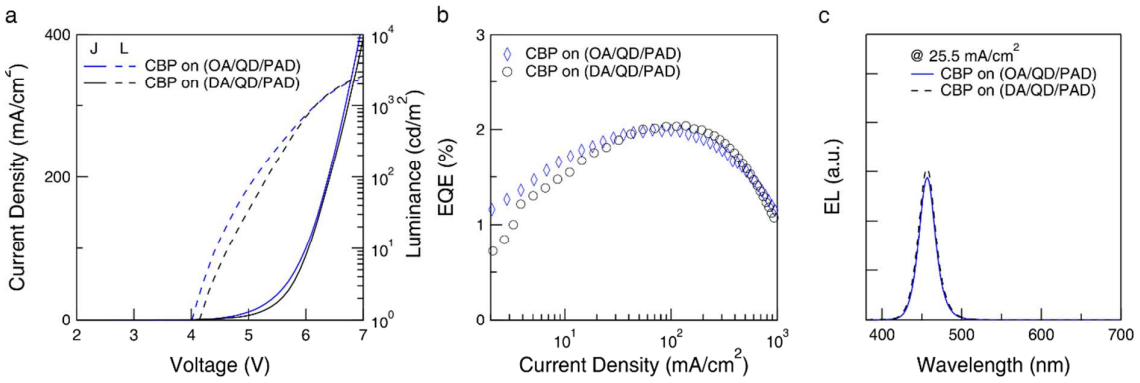

Figure S8. (a) Current density−voltage−luminance characteristics, (b) external quantum efficiency (EQE) *versus* current density and (c) electroluminescence spectra (at a current density of 25.5 mA/cm^2) of QLEDs with CBP on (OA/QD/PAD) (blue) *versus* (DA/QD/PAD) (black).

2. References

S1. Bae, W. K.; Nam, M. K.; Char, K.; Lee, S. Gram-Scale One-Pot Synthesis of Highly Luminescent Blue Emitting $Cd_{1-x}Zn_xS$/ZnS Nanocrystals. *Chem. Mater.* **2008**, *20*, 5307–5313.

S2. Pacholski, C.; Kornowski, A.; Weller, H. Self-Assembly of ZnO: from Nanodots to Nanorods. *Angew. Chem. Int. Ed.* **2002**, *41*, 1188–1191.

S3. Rudawska, A.; Jacniacka, E. Analysis for Determining Surface Free Energy Uncertainty by the Owen-Wendt Method. *Int. J. Adhes. Adhes.* **2009**, *29*, 451–457.

S4. Owens, D. K.; Wendt, R. C. Estimation of the Surface Free Energy of Polymers. *J. Appl. Polym. Sci.* **1969**, *13*, 1741–1747.

S5. http://www.sim4tec.com

S6. Kondakov, D. Y. Role of Chemical Reactions of Arylamine Hole Transport Materials in Operational Degradation of Organic Light-Emitting Diodes. *J. Appl. Phys.* **2008**, *104*, 084520.

S7. Rubstaller, B.; Carter, S. A.; Barth, S.; Riel, H.; Riess, W.; Scott, J. C. Transient and Steady-State Behavior of Space Charges in Multilayer Organic Light-Emitting Diodes. *J. Appl. Phys.* **2001**, *89*, 4575–4586.

S8. Bakhmutsky, K.; Wieder, N. L.; Cargnello, M.; Galloway, B.; Fornasiero, P.; Gorte, R. J. A Versatile Route to Core-Shell Catalysts: Synthesis of Dispersible M@Oxide (M = Pd, PT; Oxide = TiO2, ZrO2) Nanostructures by Self-Assembly. *ChemSusChem*. **2012**, *5*, 140–148.

S9. Cho, I.; Jung, H.; Jeong, B. G.; Chang, J. H.; Kim, Y.; Char, K.; Lee, D. C.; Lee, C.; Cho, J.; Bae, W. K. Multifunctional Dendrimer Ligands for High-Efficiency, Solution-Processed Quantum Dot Light-Emitting Diodes. *ACS Nano* **2017**, *11*, 684–692.